Utilization of Hydrophobic Microenvironment Sensitivity in Diethylpyrocarbonate Labeling for Protein Structure Prediction.

Sarah E. Biehn[†], Patanachai Limpikirati[‡], Richard W. Vachet[§], and Steffen Lindert[†,*]

[†]Department of Chemistry and Biochemistry, Ohio State University, Columbus, Ohio 43210

[‡]Department of Food and Pharmaceutical Chemistry, Faculty of Pharmaceutical Sciences, Chulalongkorn University, Bangkok 10330, Thailand

[§]Department of Chemistry, University of Massachusetts, Amherst, Amherst, Massachusetts 01003

*Corresponding author: lindert.1@osu.edu

ABSTRACT: Diethylpyrocarbonate (DEPC) labeling analyzed with mass spectrometry can provide important insight into higher order protein structure. It has been previously shown that neighboring hydrophobic residues promote a local increase in DEPC concentration such that serine, threonine, and tyrosine residues are more likely to be labeled despite low solvent exposure. In this work, we developed a Rosetta algorithm that used knowledge of labeled and unlabeled serine, threonine, and tyrosine residues and assessed their local hydrophobic environment to improve protein structure prediction. Additionally, DEPC-labeled histidine and lysine residues with higher relative SASA values (i.e. more exposed) were scored favorably. Application of our score term led to reductions of the root-mean-square deviations (RMSDs) of the lowest scoring models. Additionally, models that scored well tended to have lower RMSDs. A detailed tutorial describing our protocol and required command lines is included. Our work demonstrated the considerable potential of DEPC covalent labeling data to be used for accurate higher order structure determination.

With the aid of various labeling reagents, mass spectrometry (MS) is emerging as an attractive technique for investigating protein structure. Techniques such as hydrogen-deuterium exchange, chemical cross-linking, and covalent labeling have been successfully employed to elucidate protein structure and dynamics.[1-3] Covalent labeling with MS (CL-MS), in which labeling reagents irreversibly modify protein residues, can provide insight into relative solvent exposure of labeled residues. Hydroxyl radical footprinting, radical trifluoromethylation, and carbene footprinting are promising techniques in covalent labeling mass spectrometry that rely upon label generation via photolysis or radiolysis.[4-6] Diethylpyrocarbonate (DEPC) is a popular covalent labeling reagent that is commercially available; it also does not require additional steps such as radical generation.[7-9] One advantage of DEPC as a labeling reagent is the single product generation for labeled residues. DEPC reacts with six nucleophilic residues (Cys, Lys, His, Ser, Thr, and Tyr) in addition to the protein N-terminus.[7, 10,11] Labeled residues are identified by a mass increase of +72.021 Da.[12] Structures of DEPC and DEPC-modified residues are shown in Supplementary Figure 1. With careful attention to concentration and exposure times to avoid labeling-induced structural perturbation, cysteine scrambling[13] or hydrolysis leading to label loss[14], DEPC is a promising covalent labeling reagent to use for structure elucidation. While DEPC labeling yields valuable structural information, labeling data is too sparse to unambiguously determine protein structure. Computational methods are necessary in combination with the DEPC labeling data in order to illuminate additional structural detail.

MS-guided modeling has previously been successfully executed for protein structure investigation.[3, 15-23] One tool that has been applied is Rosetta, a powerful molecular modeling software suite.[24, 25] Amongst its many applications, structure prediction using sparse data from a variety of experimental techniques (including mass spectrometry) has been implemented.[24, 26-34] The Rosetta software features structural modeling applications, such as *ab initio* modeling that relies only on an amino acid sequence for structure building and template-guided homology modeling, that can predict protein structure.[25, 35] Additionally, Rosetta is capable of assessing relative solvent exposure, making it an ideal tool to predict protein structure from covalent labeling data. Functionality to use covalent labeling data to guide protein tertiary structure prediction has successfully been incorporated into the Rosetta software and shown to improve model and distribution quality.[26, 27, 29] Overall, there is a growing need for automated and reliable algorithms that generate protein structures based on CL-MS data, so as to move beyond reliance on manual interpretation of data in light of crystal structures and homology models.

Despite its ability to dissolve in aqueous solutions up to 40 mM, DEPC is a hydrophobic molecule with limited water solubility.[12, 36] Recently, it was shown that protein microenvironments enriched in neighboring hydrophobic residues led to enhanced labeling efficiency of Ser, Thr, and Tyr (STY) residues. It was proposed that nearby hydrophobic residues were facilitating an increased local concentration of DEPC, thus making STY residues more likely to be labeled.[12] Here, we exploited the connection between the microenvironmental effect of neighboring hydrophobic residues and labeling of STY residues from DEPC-based CL-MS for structural modeling. We developed a score term to assess models based on relative solvent accessible surface area (SASA) values and hydrophobic neighbor counts for labeled and unlabeled STY residues. Additionally, as more exposed residues are more likely to be covalently labeled, our score term rewarded models with labeled histidine and lysine residues that exhibited higher relative SASA values. While covalent labeling data can be difficult to accurately quantify[37, 38], we have implemented a score term that relies only upon residue DEPC-label status for structure prediction improvement. This is the first implementation of DEPC labeling data-guided structure prediction into the Rosetta software suite. When testing our algorithm on a benchmark set of six proteins, we found that inclusion of DEPC data led to lower, improved top scoring model root-mean-square deviation (RMSD) values and to an improved funnel-like quality of the model distributions.

MATERIALS AND METHODS

Benchmark set. The benchmark set was comprised of six proteins for which we obtained DEPC labeling data for His, Lys, Ser, Thr, and Tyr residues. The benchmark set included carbonic anhydrase (PDB 1V9E, 259 residues), ubiquitin (PDB 1UBQ, 76 residues), myoglobin (PDB 1DWR, 152 residues), β-2-microglobin (PDB 1JNJ, 100 residues), lysozyme (PDB 2LYZ, 129 residues), and human growth hormone (PDB 1HGU, 191 residues).

The DEPC labeling experiments and associated liquid chromatography-MS measurements were conducted as described in previous work.[12, 14, 39] For all the DEPC-protein reactions, conditions were chosen to achieve modification levels of between 1 and 1.5 labels per protein on average to maintain the structural integrity of the protein.[7, 40] Each protein was dissolved at a defined concentration between 10 and 50 μM in a 10 mM 3-(N-morpholino)propanesulfonic acid (MOPS) buffer at pH 7.4. Then, a 4- or 5-molar excess of DEPC was added and allowed to react for either 1 or 5 min. The reactions were performed at 37 °C and were quenched by the addition of imidazole. Between three and five replicates of the labeling experiments were carried out for each protein.

To enable identification of the DEPC modified residues, the labeled proteins were digested using immobilized trypsin or chymotrypsin after buffer exchange into a phosphate buffer at pH 8.0. For proteins with disulfide bonds, reduction and alkylation with a 40-fold excess of tris(2-carboxyethyl)phosphine (TCEP) and an 80-fold excess of iodoacetamide, respectively, were performed prior to digestion. Further experimental details about the digestions of ubiquitin[12], β2-microglobulin[12], human growth hormone[12], carbonic anhydrase[39], myoglobin[39], and lysozyme[41] can be found elsewhere.

The peptide fragments after protein digestion were measured by LC/MS on a Thermo Scientific (Waltham, MA) Orbitrap Fusion mass spectrometer equipped with a nano-electrospray ionization source. On-line LC separations were conducted using a Thermo Scientific Easy-NanoLC 1000 system with a Thermo Scientific Acclaim PepMap C18 nanocolumn (15 cm x 75 μm ID, 2 μm, 100 Å). Peptides were eluted using a gradient of acetonitrile containing 0.1% formic acid at a flow rate of 0.3 μL/min. The gradient of acetonitrile was increased from 0 to 50% for 50 or 60 minutes, depending on the protein digest, before ramping up the acetonitrile to 100% for 15 additional minutes. The longer acetonitrile gradient was used for the digests of carbonic anhydrase, lysozyme, and myoglobin, while the shorter gradient was used for the ubiquitin, β2-microglobin, and human growth hormone. Peptides were identified and their DEPC labeling extents were determined using a custom software pipeline[42] that allows labeling percentages as low as 0.001% to be determined. Residue level DEPC modification percentages (% labeling) were obtained from chromatographic peak areas of the unmodified and modified peptides using approaches described previously.[39] In the work described here, a residue was considered labeled if its labeling percentages exceeded 0.01%.[43]

***Ab initio* and homology model generation with Rosetta.** Fragment libraries were generated using the Robetta server for all six benchmark proteins.[44] 3mer and 9mer fragments and FASTA sequences of each benchmark proteins were used with the Rosetta *AbInitioRelax* protocol to generate 10,000 models per benchmark protein. The root-mean-square deviation (RMSD) was calculated by supplying the respective crystal structures during scoring with the Rosetta energy function (abbreviated Ref15). Models were then ranked by score. The lowest RMSD model generated was used to determine if homology modeling was necessary for the particular protein. Proteins whose lowest RMSD model exhibited an RMSD greater than 5 Å were further modeled with homology modeling.

Homology models for carbonic anhydrase, lysozyme, and human growth hormone were generated with the Rosetta Comparative Modeling protocol.[35] For each protein, seven templates (Supplementary Table 1) with varying sequence coverage (60-100%) and identity (24-99%) were used during modeling. Each template was used for the generation of 500 models for a total of 3,500 models built for each protein. Upon generation, models were relaxed with Rosetta's Relax application prior to scoring with the Rosetta Ref15 energy function and RMSD calculations.[45]

Identification of hydrophobic neighbor count and relative SASA parameters. In order to derive the values used in the score term, we developed a custom Python script to identify the hydrophobic neighboring residues of labeled and unlabeled STY residues using the benchmark crystal structures. Crystal structures were only used for the initial derivation of score term parameters. Labeling data for STY residues is included in Supplementary Table 2. Distance ($dist_{ij}$) was calculated between the hydroxyl group oxygen atom in labeled and unlabeled Ser, Thr, and Tyr (STY) residues (i) and the beta carbon in the side chain of hydrophobic residues (j). Hydrophobic neighboring residues were considered to be residue types Phe, Ile, Trp, Leu, Val, Met, Tyr, Ala, and Pro, as used previously.[12] The total contribution to the neighbor count was calculated as shown in Eq. 1.

$$\mathrm{hnc_i} = \sum_{i \neq j}^{\#\text{ hydrophobic residues}} \frac{1.0}{1+\exp\left(2 \times \left(dist_{ij} - 8\text{ Å}\right)\right)} \qquad (1)$$

A midpoint value of 8.0 Å and a steepness value of 2.0 were chosen to give a full neighbor contribution up to distances of 6 Å, the molecular dimensions of the DEPC molecule.[12] Relative SASA, the solvent accessible surface area of the residue sidechain normalized by the free residue solvent accessible surface area of the side chain, was calculated for the crystal structures using Rosetta RelSASA. Relative SASA values ranged from 0% indicating complete burial to 100% implying full exposure. A relative SASA range of 5-35% demonstrated ~1 residue difference in average neighbor count between 24 labeled and 22 unlabeled residues. Labeled HK residues are listed in Supplementary Table 3. The relative SASA for labeled HK residues was calculated using the Rosetta RelSASA application, and crystal structures of benchmark proteins were used as input structures. A relative SASA range of 65-100% was pursued as residues within this range are very solvent exposed.

To assess the noisiness of the exposure data, we investigated the number of false negatives in our datasets. False negatives were defined as unlabeled residues with high solvent exposure, and it has been shown that datasets can accommodate up to 35% false negatives data and still meaningfully guide protein structure prediction.[26] Unlabeled STY residues with 5-35% relative SASA and a high hydrophobic neighbor count were considered false negatives. We defined a high hydrophobic neighbor count as greater than 3.91, which is the midpoint between the average labeled hydrophobic neighbor count (4.42) and the average unlabeled hydrophobic neighbor count (3.39). False negatives within the 65-100% SASA HK residues were defined as unlabeled HK residues with greater than 80% SASA, the midpoint between the average labeled SASA and the averaged unlabeled SASA of HK residues. False positives were also calculated by assessing the number of labeled STY residues with hydrophobic neighbor counts less than 3.91 and labeled HK residues with relative SASA values less than 80% relative SASA. The percentage of false negatives and false positives for each residue type set was calculated using a custom Python script.

DEPC-guided scoring and model evaluation. Based on the observed differences in Ser, Thr, and Tyr labeled and unlabeled hydrophobic neighbor counts, a score term was developed to harness these variations for structure prediction. The labeled portion of the term, *STY_labeled*, was calculated using Eq. 2:

$$STY\_labeled = \sum_i^n \left[\frac{1.0}{1+\exp\left(8 \times (\mathrm{hnc}_i - 4.42)\right)} - 1\right] \quad (2)$$

in which *n* represents the number of labeled Ser, Thr, and Tyr residues, hnc_i is the hydrophobic neighbor count (see equation 1; calculated within the Rosetta score term) of the labeled Ser, Thr, or Tyr residue *i*, *8.0* is the steepness value, and *4.42* is the average hydrophobic neighbor count value calculated from the number of hydrophobic neighboring residues of labeled Ser, Thr, and Tyr residues according to the initial derivation. The per-residue *depc_ms_STY_labeled* value ranged from -1, representing agreement with the labeled residue having a hydrophobic environment, to 0, indicating disagreement because the labeled residue did not exhibit a hydrophobic environment. The unlabeled portion of the term, *STY_unlabeled*, was calculated as shown in Eq. 3:

$$STY\_unlabeled = \sum_i^n \frac{-1.0}{1+\exp\left(8 \times (\mathrm{hnc}_i - 3.39)\right)} \quad (3)$$

in which *n* is the number of unlabeled Ser, Thr, and Tyr residues, hnc_i is the hydrophobic neighbor count (calculated within Rosetta) of the particular unlabeled Ser, Thr, or Tyr residue *i*, *8.0* is the steepness value, and *3.39* is the average hydrophobic neighbor count value of unlabeled Ser, Thr, and Tyr residues in the benchmark protein crystal structures. The per-residue values also ranged from -1, indicating the unlabeled residue had fewer hydrophobic neighbors, to 0, implying that the unlabeled residue had more hydrophobic neighboring residues and disagreed with expected trends.

Labeled His and Lys residues were rewarded based on their relative SASA value, as shown in the *HK_labeled* term in Eq. 4:

$$HK\_labeled = \sum_i^n \left[\frac{1.0}{1.0+\exp\left(2.0 \times (relSASA_i - 0.65)\right)} - 1\right] \quad (4)$$

in which *n* is the number of labeled His and Lys residues, $relSASA_i$ is the relative SASA value of the labeled His or Lys residue *i*, *2.0* is the steepness value, and *0.65* is the midpoint value of the score. The midpoint value was set as the lower end of the investigated SASA range, 65-100%, which demonstrated a measurable difference in the average relative SASA value between labeled and unlabeled residues.

Finally, the labeled and the unlabeled scores for Ser, Thr, and Tyr residues along with the portion from labeled His and Lys residues were aggregated to determine *depc_ms*, as shown in Eq. 5.

$$depc\_ms = STY\_labeled + STY\_unlabeled + HK\_labeled \quad (5)$$

The *depc_ms* term was used to score 10,000 *ab initio* models (for each of the benchmark proteins β2-microglobin, ubiquitin, and myoglobin) and 3,500 homology models (for each of the benchmark proteins carbonic anhydrase, lysozyme, and human growth hormone). The total score was calculated as a weighted superposition of the initial Rosetta score and the *depc_ms* score (as shown in Eq. 6).

$$\text{Total score} = (9.0 \times depc\_ms\ score) + \text{Rosetta Ref15 score} \quad (6)$$

A weight of 9.0 was used, similar to those reported in previous work.[27, 29] A tutorial describing how to use DEPC data to predict protein structure in Rosetta is included in the Supplementary Materials section.

A comparison of Rosetta scoring and scoring with *depc_ms* was executed using several evaluation metrics. The top scoring model RMSD value was compared before and after rescoring. Additionally, the funnel-like quality, or the shape of the score versus RMSD distributions, was assessed with P_{near}. The metric P_{near} provided insight into whether the score versus RMSD distributions featured distinctive low-energy conformations that were similar to the crystal structure. We used a funnel depth of 1.0 as proposed by Bhardwaj et al and employed in our previous score term implementations.[27, 29, 46] P_{near} was calculated according to Eq. 7:

$$P_{near} = \frac{\sum_{m=1}^{n} \exp\left(-\frac{\mathrm{rmsd}_{\mathrm{m}}^2}{\lambda^2}\right)\exp\left(-\frac{\mathrm{score}_{\mathrm{m}}}{k_B T}\right)}{\sum_{m=1}^{n} \exp\left(-\frac{\mathrm{score}_{\mathrm{m}}}{k_B T}\right)}$$

in which *n* represents the number of models generated, $score_m$ is the score of the model, and $rmsd_m$ is the RMSD of the particular model to the crystal structure. The λ value was maintained at 2.0 Å to specify which models were considered native-like. k_BT, the effect of funnel depth, was maintained at a value of 1.0. A P_{near} value of 0 indicated no funnel-like quality while a value of 1 signified a perfect funnel-like distribution.

RESULTS AND DISCUSSION

Identification of relative SASA ranges to maximize differences in labeled and unlabeled residues. Based on the proposition that DEPC labeling for STY residues is sensitive to neighboring hydrophobic residues in the microenvironment,[12] we aimed to use Rosetta to elucidate a notable difference in hydrophobic neighbor count between labeled and unlabeled STY residues.

The six proteins in our benchmark set for which we obtained DEPC-based CL-MS data were carbonic anhydrase, ubiquitin, myoglobin, β2-microglobin, lysozyme, and human growth hormone. We used the crystal structures of the benchmark proteins during the score development in order to identify the number of hydrophobic neighbors in the microenvironment and relative solvent exposures of the STY residues.

We identified all STY residues with a relative SASA ranging from 5 to 35%. Within the benchmark set, this encompassed 24 labeled STY residues and 22 unlabeled STY residues. This SASA range captured low-exposure STY residues, similar to those which were noted to be relevant to hydrophobic microenvironmental effects. Subsequently, we assessed the hydrophobic microenvironment for all 46 low-exposure STY residues by measuring the hydrophobic neighbor counts.

To maintain the 6 Å distance similar to DEPC molecular dimensions[12] while still accounting for neighbors likely to have a microenvironmental effect on labeling, we used a gradual neighbor count contribution method. We calculated the per-residue neighbor count by determining the contribution of neighboring hydrophobic residues based on the distance from the STY hydroxyl group. The average labeled STY hydrophobic neighbor count was determined to be 4.42, while the average unlabeled STY hydrophobic neighbor count was 3.39, as shown in Figure 1. The violin plot in Figure 1 shows the relative frequency of hydrophobic neighbor count values for labeled and unlabeled STY residues. There were less than four hydrophobic neighbors for 46% of labeled STY residues versus 68% of unlabeled STY residues while only 25% of labeled residues and 14% of unlabeled residues had a hydrophobic neighbor count greater than five. Labeled STY residues exhibited more hydrophobic neighbors than unlabeled STY residues, corroborating that STY labeling is sensitive to neighboring hydrophobic residues within the microenvironment.

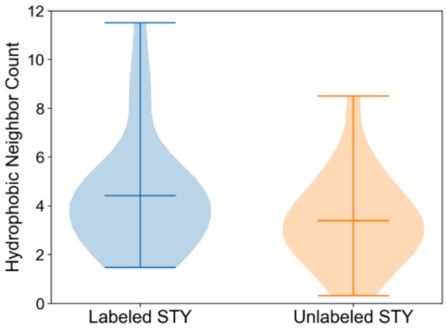

Figure 1. Violin plot demonstrating the relative frequency of different hydrophobic neighbor count values for labeled STY (blue, includes 24 residues) and unlabeled STY (orange, includes 22 residues) residues with relative SASA values of 5-35% from benchmark protein crystal structures. Mean and extrema are shown on the plot.

Using the observed trends, we developed a Rosetta score term that rewarded models containing labeled STY residues with higher hydrophobic neighbor counts and also rewarded models containing unlabeled STY residues with lower hydrophobic neighbor counts.

Additionally, since exposed His and Lys residues are more likely to be labeled by DEPC[12], we developed a score that rewarded labeled His and Lys residues with high exposure (independent of their hydrophobic neighbor count). We used a relative SASA range of 65% to 100% to reward labeled His and Lys residues with high solvent exposure. The violin plot distribution for labeled and unlabeled HK relative SASA values is shown in Supplementary Figure 2, which demonstrated the expected trend that labeled HK residues were more likely to be strongly solvent exposed. The average relative SASA for labeled residues was 0.09 higher than those of unlabeled residues. None of the unlabeled HK residues had relative SASA values greater than 0.9, while 37.5% of labeled HK residues had relative SASA higher than 0.9.

We sought to examine the noise level of DEPC labeling data by investigating false negative data points. False negative data points within covalently labeling datasets have been previously examined; it has been suggested that 35% of exposed residues can be tolerated as false negatives while still being useful for protein structure prediction.[26] We defined false negatives in this work as unlabeled STY residues with a hydrophobic neighbor count greater than 3.91 and unlabeled HK residues with relative SASAs greater than 80%. We found that 26% of the subset of STY residues with 5-35% SASA were false negatives, and 16% of the unlabeled HK residues within 65-100% SASA were false negatives. Both residue subsets fell well below the 35% tolerance cutoff, demonstrating that while some noise existed in our datasets, it did not impact our ability to predict accurate structures. False positive data points were defined as labeled STY residues with a hydrophobic neighbor count less than 3.91 and labeled HK residues with relative SASAs less than 80%. We determined that 15% of labeled STY residues with 5-35% relative SASA were false positives, and 16% of labeled HK residues with 65-100% relative SASA were false positives. Subsequently, we sought to utilize the observed exposure and microenvironment trends for STY and HK residues in Rosetta protein structure prediction.

Ab initio models scored with the DEPC-guided score term showed improvement in best scoring model RMSDs and funnel-like distributions. Based on differences in hydrophobic neighbor counts for labeled and unlabeled STY residues (Figure 1) and differences in SASA for labeled and unlabeled HK residues (Supplementary Figure 2), we proceeded to develop a score term that rewarded the desired trends. An overview of the score term is shown in Figure 2. We mapped the label status of labeled and unlabeled residues onto protein models using the DEPC-based CL-MS data. Panel 2a depicts the inputs of the score term, which included labeling data as label status (L for labeled, U for unlabeled) and appropriate residue number along with *ab initio* or homology protein models. Additional details can be found the tutorials in Supplementary Note 1. We calculated relative SASA for all mapped residues and hydrophobic neighbor counts for buried STY residues (Panel 2b). The score term included components that rewarded labeled STY residues with high numbers of hydrophobic neighbors, rewarded unlabeled STY residues with low numbers of hydrophobic neighbors, and rewarded labeled HK residues with high solvent exposure (Panel 2c). While our initial analysis of hydrophobic neighbor counts and relative SASA ranges relied on crystal structures, no crystal structures were used in model generation or score term evaluation. To test DEPC-guided scoring, we generated 10,000 *ab initio* models for each protein within our benchmark set. Upon examination of the *ab initio* models, we noticed that three of the benchmark protein model sets did not contain any models under 5 Å RMSD to the crystal structure. The DEPC score was designed to distinguish native-like models (RMSD < 5 Å) from incorrect models (RMSD > 10 Å). In order to have higher quality models present in all of the benchmark cases, homology models were generated for those three benchmark proteins. The results of scoring those homology models will be discussed in the next section.

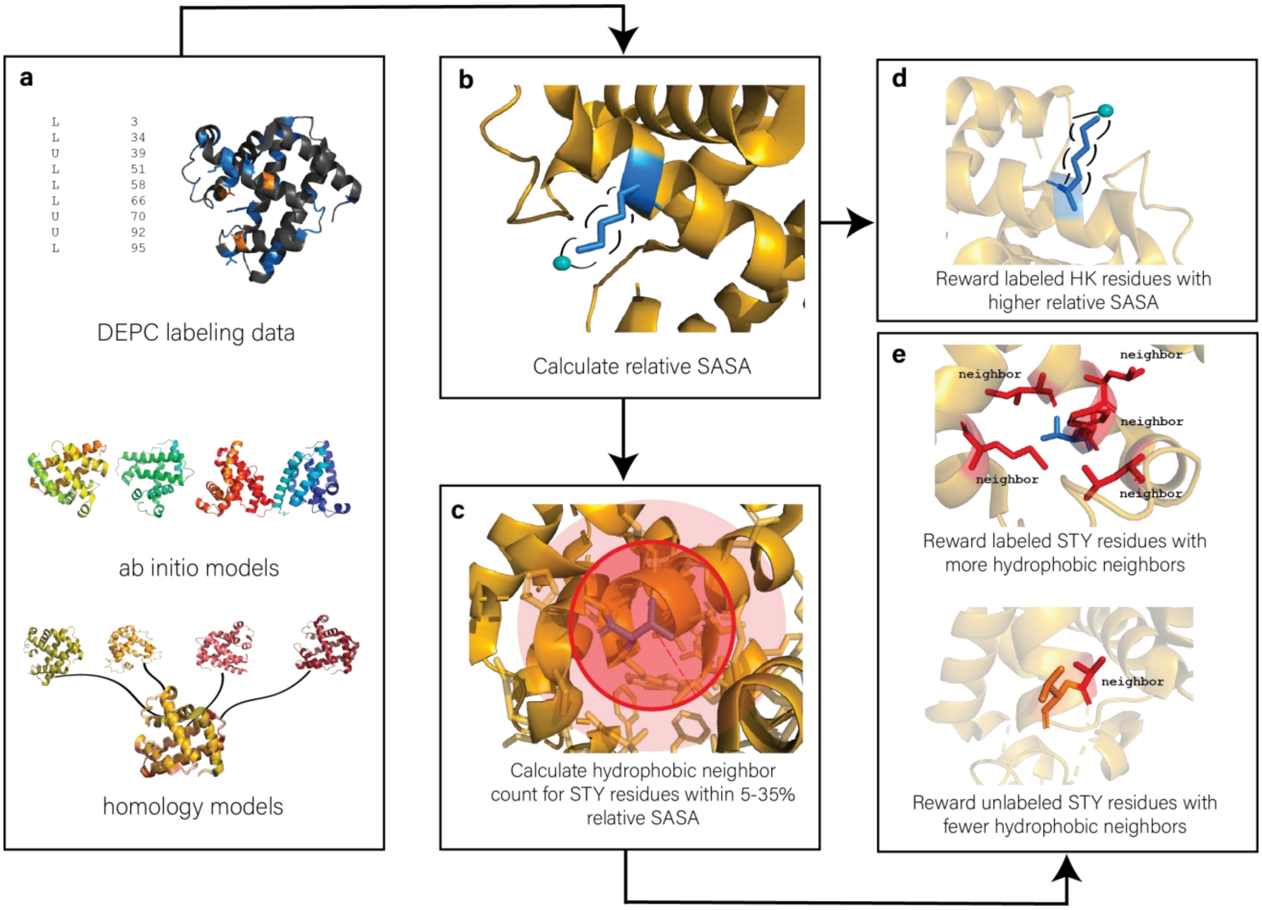
a
L 3
L 34
U 39
L 51
L 58
L 66
U 70
U 92
L 95
DEPC labeling data
ab initio models
homology models
b
Calculate relative SASA
c
Calculate hydrophobic neighbor count for STY residues within 5-35% relative SASA
d
Reward labeled HK residues with higher relative SASA
e
neighbor
neighbor
neighbor
neighbor
neighbor
Reward labeled STY residues with more hydrophobic neighbors
neighbor
Reward unlabeled STY residues with fewer hydrophobic neighbors

Figure 2. Overview of the DEPC score term (*depc_ms*) algorithm. The DEPC score term required CL-MS labeling data (residue numbers and label status) as input, along with input structures, which were either generated with homology or *ab initio* modeling (**a**). The relative SASA was calculated for all residues listed in the input file (**b**). If the residue was STY, additionally the hydrophobic neighbor count was calculated for residues with relative SASA between 5 and 35% (**c**). Labeled HK residues with higher relative SASA were rewarded (**d**). Labeled STY residues with more hydrophobic neighbors and unlabeled residues with less hydrophobic neighbors were rewarded as well (**e**).

For the three proteins whose *ab initio* model distributions included native-like models (ubiquitin, myoglobin, and β2-microglobin), we tested our score term, *depc_ms*, by adding the DEPC score to the total Rosetta score. As seen in Figure 3, the best scoring model RMSD values improved from Rosetta scoring (Figure 3a) to scoring with Rosetta and *depc_ms*, our DEPC-guided score term (Figure 3b). The RMSD of the best scoring model for β2-microglobin improved from an RMSD of 3.14 Å to 2.13 Å while ubiquitin improved from an RMSD of 3.16 Å to 1.97 Å. Myoglobin saw notable improvement from an RMSD of 7.11 Å to 1.36 Å when scoring with the *depc_ms* term.

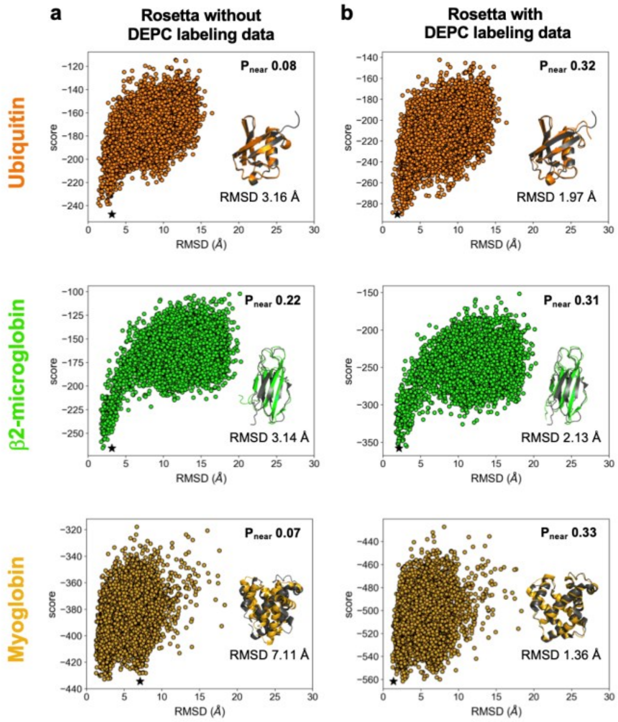

Figure 3. Score versus RMSD to the crystal structure for 10,000 *ab initio* models for a, Rosetta without DEPC labeling data and b, Rosetta with DEPC labeling data. Best scoring models are marked by a black star and shown in color aligned to the crystal structure (grey). P_{near} values are listed.

Additionally, the funnel-like quality of the distributions was quantified by the P_{near} value, with a higher P_{near} value (near 1) indicating more funnel-like quality and a lower P_{near} value (near 0) indicating lack of any funnel-like quality. We noticed that all distributions became more funnel-like, i.e. increased in P_{near}, with DEPC labeling data included in scoring, indicating that we were selecting lower-energy conformations that were more similar to the native. For β2-microglobin, P_{near} values increased from 0.22 with Rosetta to 0.31 with *depc_ms*; ubiquitin improved from 0.08 to 0.32. Myoglobin exhibited the largest improvement in P_{near} value, increasing from 0.07 to 0.33 with *depc_ms* scoring.

Homology model predictions also improved upon scoring with DEPC data. For carbonic anhydrase, human growth hormone, and lysozyme, the best model generated with *ab initio* modeling had an RMSD value greater than 5 Å to the crystal structure. We thus sought to generate additional models with Rosetta's comparative modeling protocol. The homology modeling templates with their respective sequence identities and similarities are shown in Supplementary Table 1. By generating 500 models per template and using multiple templates per protein, we were able to generate a distribution of models with varying RMSD values. We scored all models with *depc_ms* and subsequently added the score to the Rosetta score. Total score versus RMSD plots along with the best scoring model aligned with the crystal structure are shown in Figure 4. While the models identified by Rosetta were already significantly better for homology models (as compared to the *ab initio* models in the last section), scoring with DEPC data further improved model selection consistently. The human growth hormone best scoring model RMSD improved from 4.31 Å with Rosetta without labeling data to 3.85 Å with Rosetta with DEPC labeling data by way of *depc_ms*. The lysozyme best scoring model RMSD (0.78 Å) stayed constant from Rosetta to scoring with DEPC data, at already accurate atomic detail. Finally, the carbonic anhydrase best scoring model RMSD improved from 1.33 Å to 1.22 Å.

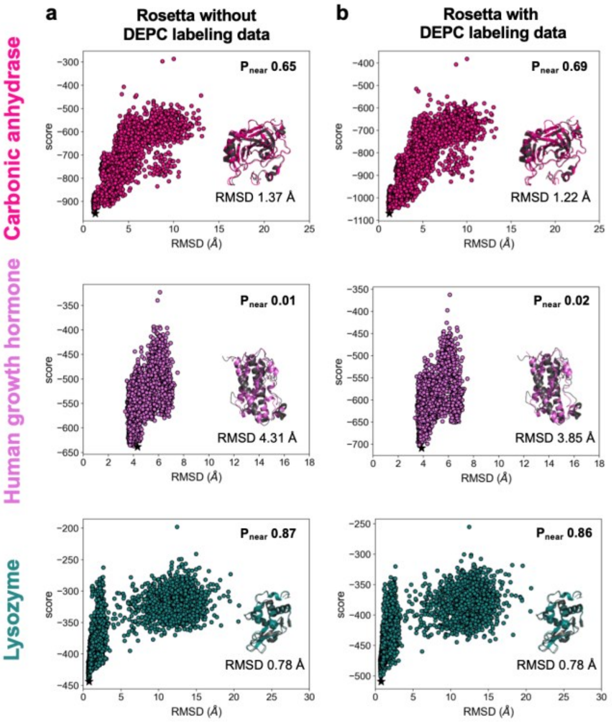

Figure 4. Score versus RMSD to the crystal structure for 3,500 homology models for a, Rosetta without DEPC labeling data and b, Rosetta with DEPC labeling data. Best scoring models are marked by a black star and shown in color aligned to the crystal structure (grey). P_{near} values are listed.

Improvements in the funnel-like quality of the distributions, P_{near}, were also noted for both human growth hormone and carbonic anhydrase. The P_{near} value of lysozyme, for which the best scoring model had a sub-angstrom RMSD, stayed at 0.83, an already near-perfect value. Human growth hormone P_{near} slightly improved from 0.01 to 0.02 while carbonic anhydrase P_{near} improved from 0.65 to 0.69 with DEPC scoring. Overall, our scoring methodology with DEPC labeling data successfully improved best scoring model quality and distribution funnel-like quality.

CONCLUSION

To employ DEPC labeling MS data in protein structure prediction, we analyzed the difference in hydrophobic neighbor counts between labeled and unlabeled STY residues and used labeled HK residues with high solvent exposure. Our benchmark set, consisting of DEPC-labeled ubiquitin, β2-microglobin, myoglobin, human growth hormone, carbonic anhydrase, and lysozyme, was used to explore the utility of DEPC labeling in protein structure elucidation. We developed a novel Rosetta score term which rewarded STY residues known to be DEPC labeled if those residues exhibited a hydrophobic microenvironment and rewarded unlabeled STY residues that lacked such hydrophobic microenvironment. Additionally, the term rewarded labeled HK residues with high solvent exposure. In a test of our algorithm, we noted that usage of DEPC data improved best scoring model RMSD and the funnel-like quality of the model distribution. For the six benchmark proteins, we saw improvement in prediction quality for both *ab initio* and homology models. Notably, we elucidated accurate atomic detail for all six proteins upon employment of DEPC labeling data. The advantageous qualities of the DEPC label, such as single product generation and ease of commercial availability, along with our DEPC-guided Rosetta modeling that is solely based on label status and computationally determined exposure metrics underscore the huge potential of DEPC labeling for protein structure determination.

While our work was primarily focused on DEPC labeling, different modeling strategies for other types of labels have previously been developed. The nature of the label generally dictates the modeling strategies warranted. For instance, hydroxyl radical protein footprinting is sufficiently modeled with solvent exposure alone.[29] Modeling HDX labeling benefits from accounting for both residue exposure and flexibility.[47] Other labels with microenvironmental effects would benefit from further analysis regarding modeling strategies to employ. Future work will continue to pursue covalent labeling data implementation into model generation protocols. Additionally, we aim to test this methodology on larger (500-1000 residues) proteins. We plan to examine the accuracy of our scoring function when utilizing DEPC data as labeling extent. Further studies will also emphasize the role of dynamics and microenvironmental effects in covalent labeling.

ASSOCIATED CONTENT

Supporting Information

The Supporting Information is available free of charge on the ACS Publications website.

DEPC-modified residue structures, violin plot comparing relative SASA between labeled and unlabeled HK residues, table of templates used for homology model generation, labeling data for STY and HK residues, and step-by-step command line tutorial for homology model generation and score term usage (PDF)

Tutorial files including 500 *ab initio* models, input files, and homology modeling script and weights (ZIP)

AUTHOR INFORMATION

Corresponding Author

*Department of Chemistry and Biochemistry, Ohio State University
2114 Newman & Wolfrom Laboratory, 100 W. 18th Avenue, Columbus, OH 43210
614-292-8284 (office), 614-292-1685 (office)
lindert.1@osu.edu

Author Contributions

P. L. and R. V. W. performed DEPC labeling experiments. S. E. B. and S. L. designed the Rosetta prediction algorithm and performed benchmark analysis. S. E. B., R. V. W., and S. L. wrote the paper.

ACKNOWLEDGMENT

The authors would like to thank the members of the Lindert and Vachet labs for useful discussions and the Ohio Supercomputer Center for computational resources.[48] Research reported in this publication was supported by NSF (CHE 1750666) to S.L. and by the NIH (R01 GM075092) to R.W.V.

REFERENCES

1. Konermann, L.; Pan, J.; Liu, Y.-H., Hydrogen exchange mass spectrometry for studying protein structure and dynamics. *Chem. Soc. Rev.* **2011,** *40* (3), 1224-1234.
2. Sinz, A., Chemical cross-linking and mass spectrometry to map three-dimensional protein structures and protein–protein interactions. *Mass Spectrom. Rev.* **2006,** *25* (4), 663-682.
3. Liu, X. R.; Zhang, M. M.; Gross, M. L., Mass Spectrometry-Based Protein Footprinting for Higher-Order Structure Analysis: Fundamentals and Applications. *Chem. Rev.* **2020,** *120* (10), 4355-4454.
4. Xu, G.; Chance, M. R., Hydroxyl radical-mediated modification of proteins as probes for structural proteomics. *Chem. Rev.* **2007,** *107* (8), 3514-3543.
5. Cheng, M.; Zhang, B.; Cui, W.; Gross, M. L., Laser-initiated radical trifluoromethylation of peptides and proteins: Application to mass-spectrometry-based protein footprinting. *Angew. Chem., Int. Ed.* **2017,** *56* (45), 14007-14010.
6. Jumper, C. C.; Schriemer, D. C., Mass spectrometry of laser-initiated carbene reactions for protein topographic analysis. *Anal. Chem.* **2011,** *83* (8), 2913-2920.
7. Limpikirati, P.; Liu, T.; Vachet, R. W., Covalent labeling-mass spectrometry with non-specific reagents for studying protein structure and interactions. *Methods* **2018,** *144*, 79-93.
8. Glocker, M.; Kalkum, M.; Yamamoto, R.; Schreurs, J., Selective biochemical modification of functional residues in recombinant human macrophage colony-stimulating factor β (rhM-CSF β): identification by mass spectrometry. *Biochemistry* **1996,** *35* (46), 14625-14633.
9. Dage, J. L.; Sun, H.; Halsall, H. B., Determination of diethylpyrocarbonate-modified amino acid residues in α1-acid glycoprotein by high-performance liquid chromatography electrospray ionization–mass spectrometry and matrix-assisted laser desorption/ionization time-of-flight–mass spectrometry. *Anal. Biochem.* **1998,** *257* (2), 176-185.
10. Mendoza, V. L.; Vachet, R. W., Probing protein structure by amino acid-specific covalent labeling and mass spectrometry. *Mass Spectrom. Rev.* **2009,** *28* (5), 785-815.
11. Mendoza, V. L.; Vachet, R. W., Protein surface mapping using diethylpyrocarbonate with mass spectrometric detection. *Anal. Chem.* **2008,** *80* (8), 2895-2904.
12. Limpikirati, P.; Pan, X.; Vachet, R. W., Covalent Labeling with Diethylpyrocarbonate: Sensitive to the Residue Microenvironment, Providing Improved Analysis of Protein Higher Order Structure by Mass Spectrometry. *Anal. Chem.* **2019,** *91* (13), 8516-8523.
13. Zhou, Y.; Vachet, R. W., Diethylpyrocarbonate labeling for the structural analysis of proteins: label scrambling in solution and how to avoid it. *J. Am. Soc. Mass Spectrom.* **2012,** *23* (5), 899-907.
14. Zhou, Y.; Vachet, R. W., Increased protein structural resolution from diethylpyrocarbonate-based covalent labeling and mass spectrometric detection. *J. Am. Soc. Mass Spectrom.* **2012,** *23* (4), 708-717.
15. Xie, B.; Sood, A.; Woods, R. J.; Sharp, J. S., Quantitative protein topography measurements by high resolution hydroxyl radical protein footprinting enable accurate molecular model selection. *Sci. Rep.* **2017,** *7* (1), 4552.

16. Benesch, J. L.; Ruotolo, B. T., Mass spectrometry: come of age for structural and dynamical biology. *Curr. Opin. Struct. Biol.* **2011,** *21* (5), 641-649.

17. Jia, R.; Martens, C.; Shekhar, M.; Pant, S.; Pellowe, G. A.; Lau, A. M.; Findlay, H. E.; Harris, N. J.; Tajkhorshid, E.; Booth, P. J., Hydrogen-deuterium exchange mass spectrometry captures distinct dynamics upon substrate and inhibitor binding to a transporter. *Nat. Commun.* **2020**, 11, 6162.

18. Murcia Rios, A.; Vahidi, S.; Dunn, S. D.; Konermann, L., Evidence for a Partially Stalled γ Rotor in F1-ATPase from Hydrogen–Deuterium Exchange Experiments and Molecular Dynamics Simulations. *J. Am. Chem. Soc.* **2018,** *140* (44), 14860-14869.

19. Hall, Z.; Politis, A.; Robinson, C. V., Structural modeling of heteromeric protein complexes from disassembly pathways and ion mobility-mass spectrometry. *Structure* **2012,** *20* (9), 1596-1609.

20. Marklund, E. G.; Degiacomi, M. T.; Robinson, C. V.; Baldwin, A. J.; Benesch, J. L., Collision cross sections for structural proteomics. *Structure* **2015,** *23* (4), 791-799.

21. Eschweiler, J. D.; Farrugia, M. A.; Dixit, S. M.; Hausinger, R. P.; Ruotolo, B. T., A structural model of the urease activation complex derived from ion mobility-mass spectrometry and integrative modeling. *Structure* **2018,** *26* (4), 599-606. e3.

22. Mistarz, U. H.; Chandler, S. A.; Brown, J. M.; Benesch, J. L.; Rand, K. D., Probing the dissociation of protein complexes by means of gas-phase h/d exchange mass spectrometry. *J. Am. Soc. Mass Spectrom.* **2019,** *30* (1), 45-57.

23. Busch, F.; VanAernum, Z. L.; Ju, Y.; Yan, J.; Gilbert, J. D.; Quintyn, R. S.; Bern, M.; Wysocki, V. H., Localization of protein complex bound ligands by surface-induced dissociation high-resolution mass spectrometry. *Anal. Chem.* **2018,** *90* (21), 12796-12801.

24. Leman, J. K.; Weitzner, B. D.; Lewis, S. M.; Adolf-Bryfogle, J.; Alam, N.; Alford, R. F.; Aprahamian, M.; Baker, D.; Barlow, K. A.; Barth, P., Macromolecular modeling and design in Rosetta: recent methods and frameworks. *Nat. Methods* **2020**, 1-14.

25. Alford, R. F.; Leaver-Fay, A.; Jeliazkov, J. R.; O'Meara, M. J.; DiMaio, F. P.; Park, H.; Shapovalov, M. V.; Renfrew, P. D.; Mulligan, V. K.; Kappel, K., The Rosetta all-atom energy function for macromolecular modeling and design. *J. Chem. Theory Comput.* **2017,** *13* (6), 3031-3048.

26. Aprahamian, M. L.; Lindert, S., Utility of Covalent Labeling Mass Spectrometry Data in Protein Structure Prediction with Rosetta. *J. Chem. Theory Comput.* **2019,** *15* (5), 3410-3424.

27. Aprahamian, M. L.; Chea, E. E.; Jones, L. M.; Lindert, S., Rosetta protein structure prediction from hydroxyl radical protein footprinting mass spectrometry data. *Anal. Chem.* **2018,** *90* (12), 7721-7729.

28. Kahraman, A.; Malmström, L.; Aebersold, R., Xwalk: computing and visualizing distances in cross-linking experiments. *Bioinformatics* **2011,** *27* (15), 2163-2164.

29. Biehn, S. E.; Lindert, S., Accurate protein structure prediction with hydroxyl radical protein footprinting data. *Nat. Commun.* **2021,** *12*, 341.

30. Harvey, S. R.; Seffernick, J. T.; Quintyn, R. S.; Song, Y.; Ju, Y.; Yan, J.; Sahasrabuddhe, A. N.; Norris, A.; Zhou, M.; Behrman, E. J., Lindert, S.; Wysocki, V. H., Relative interfacial cleavage energetics of protein complexes revealed by surface collisions. *Proc. Natl. Acad. Sci.* **2019,** *116* (17), 8143-8148.

31. Seffernick, J. T.; Harvey, S. R.; Wysocki, V. H.; Lindert, S., Predicting protein complex structure from surface-induced dissociation mass spectrometry data. *ACS Cent. Sci.* **2019,** *5* (8), 1330-1341.

32. Hartlmüller, C.; Göbl, C.; Madl, T., Prediction of protein structure using surface accessibility data. *Angew. Chem., Int. Ed.* **2016,** *55* (39), 11970-11974.

33. Seffernick, J. T.; Lindert, S., Hybrid methods for combined experimental and computational determination of protein structure. *J. Chem. Phys.* **2020,** *153* (24), 240901.

34. Leelananda, S. P.; Lindert, S., Using NMR Chemical Shifts and Cryo-EM Density Restraints in Iterative Rosetta-MD Protein Structure Refinement. *J. Chem. Inf. Model.* **2019**.

35. Song, Y.; DiMaio, F.; Wang, R. Y.-R.; Kim, D.; Miles, C.; Brunette, T.; Thompson, J.; Baker, D., High-resolution comparative modeling with RosettaCM. *Structure* **2013,** *21* (10), 1735-1742.

36. Miles, E. W., Modification of histidyl residues in proteins by diethylpyrocarbonate. *Methods Enzymol.* **1977**, 47, 431-442.

37. Ziemianowicz, D. S.; Sarpe, V.; Schriemer, D. C., Quantitative analysis of protein covalent labeling mass spectrometry data in the mass spec studio. *Anal. Chem.* **2019,** *91* (13), 8492-8499.

38. Barth, M.; Bender, J.; Kundlacz, T.; Schmidt, C., Evaluation of NHS-Acetate and DEPC labelling for determination of solvent accessible amino acid residues in protein complexes. *J. Proteomics* **2020,** *222*, 103793.

39. Liu, T.; Limpikirati, P.; Vachet, R. W., Synergistic Structural Information from Covalent Labeling and Hydrogen–Deuterium Exchange Mass Spectrometry for Protein–Ligand Interactions. *Anal. Chem.* **2019,** *91* (23), 15248-15254.

40. Pan, X.; Limpikirati, P.; Chen, H.; Liu, T.; Vachet, R. W., Higher-Order Structure Influences the Kinetics of Diethylpyrocarbonate Covalent Labeling of Proteins. *J. Am. Soc. Mass Spectrom.* **2020,** *31* (3), 658-665.

41. Liu, T.; Marcinko, T. M.; Vachet, R. W., Protein-ligand affinity determinations using covalent labeling-mass spectrometry. *J. Am. Soc. Mass Spectrom.* **2020**.

42. Borotto, N. B.; Zhou, Y.; Hollingsworth, S. R.; Hale, J. E.; Graban, E. M.; Vaughan, R. C.; Vachet, R. W., Investigating therapeutic protein structure with diethylpyrocarbonate labeling and mass spectrometry. *Anal. Chem.* **2015,** *87* (20), 10627-10634.

43. Limpikirati, P.; Hale, J. E.; Hazelbaker, M.; Huang, Y.; Jia, Z.; Yazdani, M.; Graban, E. M.; Vaughan, R. C.; Vachet, R. W. Covalent labeling and mass spectrometry reveal subtle higher order structural changes for antibody therapeutics. *MAbs* **2019**, 11(3), 463-476.

44. Kim, D. E.; Chivian, D.; Baker, D., Protein structure prediction and analysis using the Robetta server. *Nucleic Acids Res.* **2004,** *32* (suppl_2), W526-W531.

45. Conway, P.; Tyka, M. D.; DiMaio, F.; Konerding, D. E.; Baker, D., Relaxation of backbone bond geometry improves protein energy landscape modeling. *Protein Sci.* **2014,** *23* (1), 47-55.

46. Bhardwaj, G.; Mulligan, V. K.; Bahl, C. D.; Gilmore, J. M.; Harvey, P. J.; Cheneval, O.; Buchko, G. W.; Pulavarti, S. V.; Kaas, Q.; Eletsky, A., Accurate de novo design of hyperstable constrained peptides. *Nature* **2016,** *538* (7625), 329-335.

47. Marzolf, D. R.; Seffernick, J. T.; Lindert, S., Protein Structure Prediction from NMR Hydrogen–Deuterium Exchange Data. *J. Chem. Theory Comput.* **2021,** *17* (4), 2619-2629.

48. *Ohio Supercomputer Center*, 1987.

Insert Table of Contents artwork here

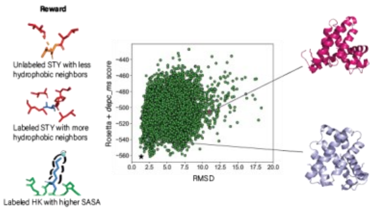
Reward
Unlabeled STY with less hydrophobic neighbors
Labeled STY with more hydrophobic neighbors
Labeled HK with higher SASA
Rosetta + depc_ms score
RMSD